Neuroprotective effects of 5-S-GAD against oxidative stress-induced apoptosis in RGC-5 cells

Neuroprotective effects of 5-S-GAD against oxidative stress-induced apoptosis in RGC-5 cells

Yoshiki Koriyama[a], Mamoru Ohno[b], Takahiro kimura[b], Satoru Kato[a]*

[a]Department of Molecular Neurobiology, Graduate School of Medicine, Kanazawa University, 13-1 Takaramachi, Kanazawa 920-8640, Japan

[b]Teika Pharmaceutical Co., Ltd., Toyama 930-0982, Japan

Number of text pages: 22

Numbers of figures: 6

*Correspondence should be addressed to:

Satoru Kato, Department of Molecular Neurobiology, Graduate School of Medicine,

Kanazawa University, 13-1 Takara-machi, Kanazawa, Ishikawa 920-8640, Japan

Tel: +81-76-265-2450, Fax: +81-76-234-4235

E-mail: satoru@med.kanazawa-u.ac.jp

Abbreviations:

4-HNE, 4-hydroxy-2-nonenal; 5-S-GAD, N-β-alanyl-5-S-glutathionyl-3,4-dihydroxyphenylalanine; CM-H_2DCFDA, 5,6-chloromethyl-2,7-dichlorodihydrofluorescein diacetate acetyl ester; DAB, 3-diaminobendizine tetrahydrochloride; FBS, fetal bovine serum; HBSS, Hanks balanced salt solution; MTT, 3-(4,5-dimethylthiazol-2-yl)-2,5-diphenyltetrazolium bromide; NMDA, N-methyl-D-aspartate; PBS, phosphate buffered saline; RGC, retinal ganglion cell; RGC-5, retinal ganglion cell-5, ROS, reactive oxygen species

Abstract

N-β-alanyl-5-S-glutathionyl-3,4-dihydroxyphenylalanine (5-S-GAD), an antibacterial substance isolated from the flesh fly, has been described as having multipotential biological activities toward various tissues. In a previous paper, we reported a novel neuroprotective action of 5-S-GAD on rat retinal ganglion cell apoptosis induced by optic nerve injury and intraocular N-methyl-D-aspartate treatment *in vivo*. In the present study, we further investigated the protective mechanism of this small peptide against other types of apoptosis in cultured cells of the established rat retinal ganglion cell line RGC-5. Hydrogen peroxide and serum deprivation treatments induced intracellular reactive oxygen species levels and lipid peroxidation, revealed by 4-hydroxy-2-nonenal production, in RGC-5 cells within 9-12 h. The treatments also induced cell death accompanied by nuclear condensation, DNA laddering and increases in apoptotic Bax and caspase-3 proteins in RGC-5 cells within 12-24 h. 5-S-GAD at 25-50 μM clearly suppressed the cell death and apoptotic features induced by these treatments. 5-S-GAD restored the nuclear condensation, DNA laddering and increases in apoptotic proteins. Furthermore, 5-S-GAD directly activated anti-apoptotic phospho-Akt and Bcl-2 proteins in RGC-5 cells. 5-S-GAD also quenched the reactive oxygen species production and inhibited the lipid peroxidation induced by oxidative stress. Therefore, 5-S-GAD may complementarily protect RGC-5 cells against apoptosis through dual actions as a radical scavenger and an inducer of anti-apoptotic phospho-Akt and Bcl-2. Taken together, 5-S-GAD is a high-potential tool for rescuing the retinal ganglion cell apoptosis induced by a variety of glaucomatous conditions.

Keywords;

Retinal ganglion cell, 5-S-GAD, neuroprotection, oxidative stress, apoptosis, glaucoma

1. Introduction

Retinal ganglion cells (RGCs) play key roles in integrating visual information and relaying it to the visual center of the brain through the optic nerve. Apoptosis of RGCs is known to be a fundamental pathogenesis in a variety of retinal degenerative diseases, such as glaucoma and diabetic retinopathy (Quigley et al. 1995; Barber et al. 1998; Lafuente et al. 2001). Several common mechanisms, such as excitotoxicity, oxidative stress ischemia and deficiency of trophic factors, have been proposed to be involved in RGC apoptosis (Wadia et al. 1998; Pease et al. 2000; Maher and Hanneken 2005). To further elucidate the molecular mechanism of RGC apoptosis, a transformed rat RGC cell line, RGC-5, was recently established (Krishnamoorthy et al. 2001). The signaling pathways leading to RGC apoptosis have been studied under glaucomatous and diabetic conditions using this cell line (Tatsumi et al. 2008; Nakajima et al. 2008). In a previous study, we showed that a novel small peptide, N-β-alanyl-5-S-glutathionyl-3,4-dihydroxyphenylalanine (5-S-GAD), protects against cell death of rat RGCs after treatment with N-methyl-D-aspartate (NMDA) or optic nerve injury in *in vivo* models (Koriyama et al. 2008). 5-S-GAD was originally isolated from the adult flesh fly as a defense substance produced in response to bacterial injection or body injury (Leem et al. 1996). 5-S-GAD inhibits the cell growth of some human tumor cells *in vitro* (Akiyama et al. 2000) and angiogenesis of mouse 8180 sarcoma cells *in vivo* (Nishikawa et al. 2006). The exact mechanism of the actions of 5-S-GAD on various types of cells and tissues has remained unclear. In the present study, we aimed to clarify the neuroprotective actions of 5-S-GAD on rat RGC apoptosis by investigating its effects on the cell death of RGC-5 cells in oxidative stress and trophic support interruption models. 5-S-GAD (25 or 50 μM) significantly prevented RGC-5 cells from undergoing cell death induced by hydrogen peroxide exposure and serum deprivation. 5-S-GAD clearly quenched the production of peroxide radicals and inhibited lipid peroxidation. Furthermore, 5-S-GAD directly activated anti-apoptotic phospho-Akt and Bcl-2 proteins in RGC-5 cells.

Therefore, 5-S-GAD may complementarily protect RGC-5 cells against apoptosis through dual actions as a radical scavenger and an activator of anti-apoptotic phospho-Akt and Bcl-2. The present data indicate that 5-S-GAD represents a therapeutic option for optic nerve neuropathies such as glaucoma.

2. Results

←---Fig. 1

2.1. 5-S-GAD protects against RGC-5 cell death induced by oxidative stress

The cell death of cultured RGC-5 cells was evaluated using an MTT reduction assay. First, we investigated the effects of 5-S-GAD on the cell viability of RGC-5 cells cultured for 24 h. 5-S-GAD alone did not affect the cell viability at concentrations of 5-50 μM (Fig. 1A). Therefore, we used 5-S-GAD at concentrations of 5-50 μM in our subsequent experiments. Next, we investigated the effects of 5-S-GAD on the neurotoxicity induced by hydrogen peroxide exposure and serum deprivation conditions in RGC-5 cells. Exposure to hydrogen peroxide (300-600 μM) clearly induced cell death in one-half of the cells within 24 h (Fig. 1A). 5-S-GAD suppressed the cell death induced by 300 μM hydrogen peroxide in a dose-dependent manner. 5-S-GAD at 50 μM completely suppressed the cell death induced by hydrogen peroxide to the level of the control cells (Fig. 1A). Serum deprivation rapidly induced cell death in more than one-half of the RGC-5 cells within 24 h (Fig. 1B). 5-S-GAD also protected against the cell death induced by serum deprivation in a dose-dependent manner. 5-S-GAD at 50 μM completely inhibited the cell death induced by serum deprivation to the level of the control cells (Fig. 1B).

←---Fig. 2

2*.2. 5-S-GAD protects against RGC-5 cell apoptosis induced by oxidative stress*

RGC-5 cells treated with 300 μM hydrogen peroxide for 24 h were stained with Hoechst 33258. RGC-5 cells treated with hydrogen peroxide showed nuclear chromatin condensation following staining with Hoechst 33258 (Fig. 2B) relative to the control cells (Fig. 2A). 5-S-GAD (50 μM) clearly suppressed the nuclear condensation induced by hydrogen peroxide (Fig. 2C). Quantification of the staining confirmed protective effects of 25-50 μM 5-S-GAD on the nuclear condensation induced by 300 μM hydrogen peroxide in RGC-5 cells (Fig. 2D), whereas 5-S-GAD alone had no

effect on the nuclear condensation. Furthermore, nuclear DNA extracted from RGC-5 cells treated with hydrogen peroxide for 24 h was subjected to electrophoresis (Fig. 2E), and exhibited a DNA fragmentation pattern (Fig. 2E, lane H) compared with nuclear DNA extracted from control cells (Fig. 2E, lane C). 5-S-GAD significantly inhibited the DNA fragmentation (Fig. 2E, lane HG). 5-S-GAD alone had no effect on the DNA fragmentation in RGC-5 cells (Fig. 2E, lane G).

←---Fig. 3

2.3. 5-S-GAD decreases the fluorescence intensity in hydrogen peroxide treated RGC-5 cells

RGC-5 cells were incubated with the fluorescent dye CM-H_2DCFDA, a trapping marker for ROS production. After 9 h in culture, 300 μM hydrogen peroxide increased fluorescence intensity including hydrogen peroxide itsekf (Nakajima et al., 2009) by 1.75-fold relative to the control cells (compare Fig. 3D-F with Fig. 3A-C; Fig. 3J). 5-S-GAD (50 μM) completely blocked the increase in fluorescence intensity induced by hydrogen peroxide (Fig. 3G-I). 5-S-GAD alone had no effect on the ROS levels in RGC-5 cells (Fig. 3J).

←---Fig. 4

2.4. 5-S-GAD protects against ROS production and DNA fragmentation induced by serum deprivation in RGC-5 cells

Similarly, we used CM-H_2DCFDA staining to investigate the effects of 5-S-GAD on the ROS production induced by serum deprivation. After 9 h in culture under serum deprivation conditions, many fluorescent cells were observed compared with control cells (compare Fig. 4D-F with Fig. 4A-C). 5-S-GAD clearly blocked the fluorescence intensity induced by serum deprivation (Fig. 4G-1). 5-S-GAD at 50 μM completely blocked the ROS production induced by serum deprivation (Fig. 4J). Furthermore, 5-S-GAD completely blocked the DNA fragmentation (Fig. 4K, compare lane SG with lane S) to a similar level to the control cells (Fig. 4K, lane C).

←---Fig. 5

2.5. 5-S-GAD protects against lipid peroxidation induced by oxidative stress in RGC-5 cells

4-HNE is a final product of lipid peroxidation (Lim et al. 2006). Therefore, we investigated the effects of 5-S-GAD on lipid peroxidation by dot blot analyses using an anti-4-HNE antibody. After 12 h in culture, hydrogen peroxide at 300 μM significantly increased the level of 4-HNE production by 1.7-fold relative to the control cells (Fig. 5A). 5-S-GAD dose-dependently suppressed the increase in 4-HNE induced by hydrogen peroxide. 5-S-GAD at 50 μM completely blocked the lipid peroxidation (Fig. 5A), whereas 5-S-GAD alone had no effect on the production of 4-HNE. Similarly, 5-S-GAD suppressed the increase in lipid peroxidation induced by serum-free conditions (Fig. 5B). The intensities of the β-actin spots remained unchanged by these treatments.

←---Fig. 6

2.6. 5-S-GAD directly activates anti-apoptotic phospho-Akt and Bcl-2 in RGC-5 cells

Since 5-S-GAD actually prevented the apoptotic features induced by hydrogen peroxide and serum deprivation as described above, we investigated the effects of 5-S-GAD on cell death and cell survival signal expressions under hydrogen peroxide exposure. Hydrogen peroxide clearly increased the levels of Bax by 1.5-fold and caspase-3 by 1.8-fold within 12 h (Fig. 6A, upper bands and 6B, respectively). 5-S-GAD reversed the hydrogen peroxide-induced increases in the levels of Bax and caspase-3 expression to the levels in control cells. In contrast, hydrogen peroxide decreased the levels of anti-apoptotic proteins to 30% of the control for phospho-Akt and 75% of the control for Bcl-2 within 12 h (Fig. 6C, upper bands and 6D, respectively). 5-S-GAD reversed the hydrogen peroxide-induced decreases in the levels of phospho-Akt and Bcl-2 to the levels in control cells. Furthermore, 5-S-GAD directly activated phospho-Akt by 1.5-fold and Bcl-2 by 1.2-fold in RGC-5 cells within 12 h (Fig. 6C, upper bands and 6D, respectively). The levels of β-actin bands were not changed during this treatment (Fig. 6A, lower bands). Levels of non-active form of Akt protein did not change during this treatment (Fig. 6C, lower). These data indicate that 5-S-GAD activates

anti-apoptotic proteins and thereby reverses the increases in apoptotic proteins after hydrogen peroxide exposure.

3. Discussion

3.1. 5-S-GAD protects RGC-5 cells against apoptosis induced by oxidative stress

Based on our previous data for rat RGCs after optic nerve injury or NMDA treatment *in vivo* (Koriyama et al. 2008), the question arose as to whether 5-S-GAD protects RGCs against the apoptosis induced by other types of insults. The eye has a 3-4-fold higher oxygen consumption than brain tissue and consequently has a high risk of exposure to various types of oxygen radicals, such as hydroxy radicals, hydrogen peroxide and superoxide anions. This is the reason why the eye is a unique tissue that contains very high quantities of anti-oxidants, such as superoxide dismutase, catalase, ascorbate and vitamin E (Rao et al. 1985; Rao 1990; Atalla et al. 1987). In the present study, we chose to examine oxidative stress and trophic support interruption treatments to evaluate the neuroprotective action of 5-S-GAD on RGC apoptosis. We used the established rat RGC cell line RGC-5 as a model cell type for RGCs (Krishnamoorthy et al. 2001). As a model of oxidative stress, we treated RGC-5 cells with hydrogen peroxide. Hydrogen peroxide at a concentration of 300 μM is sufficient to induce cell damage, including apoptosis (Nakajima et al. 2008). As a model of trophic support interruption, we cultured RGC-5 cells under serum deprivation. Both treatments are well characterized to induce RGC-5 cell apoptosis (Charles et al. 2005; Tatsumi et al. 2008). 5-S-GAD at 25-50 μM almost completely blocked the hydrogen peroxide-induced RGC-5 cell apoptosis, as evaluated by the MTT cell viability assay, nuclear condensation, DNA laddering and increases in Bax and caspase-3 within 24 h. 5-S-GAD also blocked the ROS levels and inhibited lipid peroxidation in RGC-5 cells, as evaluated by increases in CM-H_2DCFDA fluorescence and 4-HNE production within 12 h. In the case of hydrogen peroxide treated cells, CM-H_2DCFDA detected not only ROS production but also hydrogen peroxide itself. However, GAD significantly suppressed the levels of fluorescence intensity by hydrogen peroxide treatment.

Charles et al. (2005) studied the signal cascade for RGC-5 cell apoptosis under serum deprivation

conditions. They demonstrated that serum deprivation induces an increase in malonylaldehyde, a decrease in reduced glutathione and dysfunction of mitochondria leading to caspase-3 activation. 5-S-GAD at 25-50 μM similarly blocked the serum deprivation-induced RGC-5 cell apoptosis. 5-S-GAD inhibited the apoptotic features, as well as ROS production and lipid peroxidation. Our data strongly suggest that 5-S-GAD has a wide protective spectrum against the RGC apoptosis induced by oxidative stress and trophic deficiency in the present study and by optic nerve injury and NMDA treatment in our previous study (Koriyama et al. 2008). However, the concentrations of 5-S-GAD used in the previous *in vivo* study (0.2-2 pmol) and the present *in vitro* study (25-50 μM) are different. It may be due to the big differences in the experimental conditions, particularly the duration of the 5-S-GAD exposure.

3.2. Possible mechanism for the neuroprotective actions of 5-S-GAD toward RGC apoptosis

In a previous paper (Koriyama et al. 2008), we reported that intraocular 5-S-GAD activates phospho-Akt by 2.0-fold and Bcl-2 by 1.8-fold in rat RGCs at 1-3 days and 3-5 days after treatment, respectively. The second question that arose from that study was whether the activation of anti-apoptotic proteins by 5-S-GAD is direct or indirect in RGCs. The present data clearly showed that these effects were direct. 5-S-GAD induced low, but significant, activation of phospho-Akt by 1.5-fold and Bcl-2 by 1.2-fold in RGC-5 cells within 12 h. The magnitudes of the phospho-Akt and Bcl-2 activation levels differed between the *in vivo* and *in vitro* situations. This may also be due to the big differences in the experimental conditions. 5-S-GAD almost recovered the phospho-Akt and Bcl-2 levels from the decreased levels after hydrogen peroxide treatment. 5-S-GAD also recovered the phospho-Akt and Bcl-2 levels from the decreased levels induced by serum deprivation (data not shown). These results suggest that the restoration of the phospho-Akt level in RGC-5 cells is caused by the activation of anti-apoptotic proteins by 5-S-GAD. However, the restoration of ROS

production and lipid peroxidation by 5-S-GAD did not seem to be caused by this activation of anti-apoptotic proteins.

Recently, Akiyama et al. (2009) reported a novel radical scavenging action of 5-S-GAD. They clearly demonstrated that 5-S-GAD scavenges 1.1-diphenylpicrylhydrazyl and superoxide anion radical, and inhibits lipid peroxidation. The effective dose of 5-S-GAD for scavenging the free radicals and inhibiting the lipid peroxidation is ~50 μM, which is in the same order in magnitude as that in the present study. They also showed that 5-S-GAD inhibits the onset of glucocorticoid-induced lens opacification in the chick (Akiyama et al. 2009). If the radical scavenging action of 5-S-GAD is applicable to the present study, the protective actions of 5-S-GAD toward RGC-5 cell apoptosis can be fully explained by complementation of the activation of anti-apoptotic proteins. Therefore, the neuroprotective mechanism of 5-S-GAD is composed of dual actions, one as an inducer of the anti-apoptotic proteins phospho-Akt and Bcl-2 and the other as a radical scavenger. Although we do not know the exact radical species generated under serum deprivation and hydrogen peroxide treatments, 5-S-GAD effectively quenched ROS production and inhibited lipid peroxidation. The pathogenesis of RGC apoptosis induced by optic nerve injury and NMDA treatment *in vivo* is also well known to involve ROS generation (Castagné et al. 1996; El-Remessy et al. 2003; Inomata et al. 2006). Taken together, the findings in the previous *in vivo* and present *in vitro* studies strongly indicate that 5-S-GAD is one of the high-potential tools for rescuing RGC apoptosis caused by a variety of glaucomatous conditions.

4. Experimental procedures

4.1. Cell culture

RGC-5 cells were kindly gifted by Dr. N. Agarwal, University of North Texas Health Science Center and Dr. H. Hara, Gifu Pharmaceutical University. RGC-5 cells were cultured in low-glucose Dulbecco's modified Eagle's medium (DMEM) containing 10% fetal calf serum (FBS), 100 U/ml penicillin and 100 μg/ml streptomycin in a humidified atmosphere of 95% air and 5% CO_2 at 37°C. The cells were passaged by trypsinization every 3-4 days.

4.2. Cell treatments

RGC-5 cells (5×10^3 cells/ml) were cultured overnight as described above. After washing with DMEM, the cells were divided into three groups: (1) control group: (2) hydrogen peroxide-treated group; and (3) serum deprivation group. Control and the hydrogen peroxide-treated group were cultured in medium containing 1% FBS to reduce cell growth as much as possible (Nakajima et al. 2008), whereas the serum deprivation groups were cultured in serum-free medium. 5-S-GAD was a generous gift from Dr. S. Natori, RIKEN. The protective effects of 5-S-GAD were analyzed after simple addition of hydrogen peroxide or serum deprivation treatment. The cells were pretreated with 5-S-GAD for 1 h before hydrogen peroxide or serum deprivation loading.

4.3. MTT assay

The cell death was estimated using a 3-(4,5-dimethylthiazol-2-yl)-2,5-diphenyltetrazolium bromide (MTT) reduction assay. An aliquot (20 μl) of 2.75 mg/ml MTT in phosphate-buffered saline (PBS) was added to 200 μl of each culture medium as described previously (Koriyama et al. 2003).

The reaction mixtures were incubated at 37°C for 3 h, prior to the addition of 200 μl HCl/isopropanol. The produced formazan was measured by its absorbance at 550 nm using a plate reader (Model 680, Bio-Rad Laboratories, Hercules, CA). The experiments were repeated at least three times and compared with control experiments.

4.4. Nuclear staining with Hoechst 33258

Cultured RGC-5 cells were washed twice with PBS and fixed with 0.1% glutaraldehyde in PBS at room temperature for 15 min. After the fixation, the cells were washed and incubated with Hoechst 33258 (Wako; 100 μg/ml in PBS) at room temperature for 15 min. The cells with chromatin condensation were observed and counted in 25 visual fields/dish by fluorescence microscopy.

4.5. DNA fragmentation

Cultured RGC-5 cells were collected, suspended in PBS and centrifuged at 400 × *g* for 10 min. The cell pellet was resuspended and lysed in a lysis buffer (Tris-HCl pH 8.0, 10 mM NaCl, 10 mM EDTA, 1% SDS). The lysed samples were treated with RNase (0.4 μg/ml) and proteinase K (0.625 mg/ml) for 1 h at 37°C. Agarose gel (2%) electrophoresis of the isolated DNA was performed in 40 mM Tris-HCl buffer (pH 8.0) containing 2 mM EDTA, and the DNA bands were visualized after staining with ethidium bromide (0.5 μg/ml) for 15 min at room temperature.

4.6. Measurement of reactive oxygen species (ROS)

The fluorescent probe 5,6-chloromethyl-2,7-dichlorodihydrofluorescein diacetate acetyl ester (CM-H_2DCFDA; Molecular Probes) is a cell-permeable indicator of ROS (Shimazawa et al. 2005). RGC-5 cells were cultured for 9 h, washed twice with Hanks balanced salt solution (HBSS) and treated with CM-H_2DCFDA (10 μM) for 1 h at 37°C. The samples were then centrifuged at 100 × *g*

for 5 min at room temperature. The supernatants were discarded and 800 μl of HBSS was added to each cell pellet. The fluorescence intensity of each cell suspension was measured by the emission at 520 nm after excitation at 485 nm using a Fluoroskan Ascent plate reader (Thermo Labsystem) . The total cell number was evaluated by Hoechst 33258 nuclear staining.

4.7. Western blotting analysis

RGC-5 cells cultured under various conditions for 12 h were extracted and aliquots (15 μg of protein) were subjected to SDS-PAGE using a 12.5% gel as described previously (Koriyama et al. 2003). The separated proteins were transferred to a nitrocellulose membrane and incubated with primary and secondary antibodies as described previously (Koriyama et al. 2007). The signals for the antibody-bound protein bands (28 kDa for Bax; 26 kDa for Bcl-2; 17 kDa for active caspase-3; 56 kDa for phospho-Akt) were detected using 3-diaminobendizine tetrahydrochloride (DAB) as a substrate. An antibody against β-actin was used as an internal standard. The protein bands produced by samples from cells under various culture conditions were analyzed densitometrically using the Scion Image Software (Scion Corp.). All experiments were repeated at least three times.

4.8. Dot blotting analysis for 4-hydroxy-2-nonenal (4-HNE)

After the western blot analysis, equal amounts of protein (15 μg) were applied to a Hybri-SLOT apparatus (Gibco BRL) and transferred to a nitrocellulose membrane (Whatman) by vacuum filtration. After blocking with 3% BSA for 1 h at room temperature, the samples were incubated with an anti-4-HNE antibody (1:100; NOF Corporation) for 12 h at 4°C, followed by incubation with a peroxidase-conjugated anti-mouse IgG antibody (1:500, Santa Cruz Biotechnology, CA, USA) for 1 h at room temperature. Antibody-bound protein bands were detected using DAB as a substrate and analyzed densitometrically as described above. All experiments were repeated at least three times.

4.9. Statistical analysis

The values for the cell death, number of positively stained cells with fluorescence probe and densitometrically analyzed protein bands were calculated as the means ± SEM from 3-5 independent experiments. Statistical significance was determined as values of $P<0.05$ using one-way ANOVA followed by multiple comparisons by Dunnett's test.

Acknowledgments

We thank Ms Tami Urano, Ms Sachiko Higashi and Ms Tomoko Kano for administrative and technical assistance. This work was partly supported by research grants from Ministry of Education, Science, Sports and Culture (Nos 18209053, 1965447 to SK; 19700338 to YK) from Kanazawa University Awards for Young Scientist to YK (2006, 2007, 2008) and from Research for Promoting Technological Seeds, Japan Science and Technology Agency (JST) 2009 to YK.

References

Akiyama, N., Hijikata, M., Kobayashi, A., Yamori, T., Tsuruo, T., Natori, S. 2000. Anti-tumor effect of N-beta-alanyl-5-S-glutathionyldihydroxyphenylalanine (5-S-GAD), a novel anti-bacterial substance from an insect. Anticancer Res. 20. 357-362.

Akiyama, N., Umeda, I.O., Sogo, S., Nishigori, H., Tsujimoto, M., Natori, S. 2009. 5-S-GAD, a novel radical scavenging compound, prevents lens opacity development. Free Radic. Biol. Med. 46. 511-519.

Atalla, L., Fernandez, M., Rao, N.A 1987. Immunohistochemical localization of catalase in ocular tissue. Curr. Eye Res. 6, 1181-1187.

Barber, A.J., Lieth, E., Khin, S.A., Antonetti, D.A., Buchanan, A.G., Gardner, T.W., 1998. Neural apoptosis in the retina during experimental and human diabetes. Early onset and effect of insulin. J. Clin. Invest. 102, 783-791.

Castagné, V., Clarke, P.G. 1996. Axotomy-induced retinal ganglion cell death in development: its time-course and its diminution by antioxidants. Proc. Biol. Sci. 263, 1193-1197.

Charles, I., Khalyfa, A., Kumar, D.M., Krishnamoorthy, R.R., Roque, R.S., Cooper, N., Agarwal, N. 2005. Serum deprivation induces apoptotic cell death of transformed rat retinal ganglion cells via mitochondrial signaling pathways. Invest. Ophthalmol. Vis. Sci. 46. 1330-1338.

El-Remessy, A.B., Khalil, I.E., Matragoon, S., Abou-Mohamed, G., Tsai, N.J., Roon, P., Caldwell, R.B., Caldwell, R.W,. Green, K., Liou, G.I. 2003. Neuroprotective effect of (-)Delta9-tetrahydrocannabinol and cannabidiol in N-methyl-D-aspartate-induced retinal neurotoxicity: involvement of peroxynitrite. Am. J. Pathol. 163, 1997-2008.

Inomata, Y., Nakamura, H., Tanito, M., Teratani, A., Kawaji, T., Kondo, N., Yodoi, J., Tanihara, H. 2006. Thioredoxin inhibits NMDA-induced neurotoxicity in the rat retina. J. Neurochem. 2006. 98. 372-385.

Koriyama, Y., Chiba, K., Mohri, T. 2003. Propentofylline protects beta-amyloid protein-induced apoptosis in cultured rat hippocampal neurons. Eur. J. Pharmacol. 458. 235-241.

Koriyama, Y., Homma, K., Sugitani, K., Higuchi, Y., Matsukawa, T., Murayama, D., Kato, S. 2007. Upregulation of IGF-I in the goldfish retinal ganglion cells during the early stage of optic nerve regeneration. Neurochem. Int. 50. 749-756.

Koriyama, Y., Tanii, H., Ohno, M., Kimura, T., Kato, S. 2008. A novel neuroprotective role of a small peptide from flesh fly, 5-S-GAD in the rat retina in vivo. Brain Res. 1240, 196-203.

Krishnamoorthy, R.R., Agarwal, P., Prasanna, G., Vopat, K., Lambert, W., Sheedlo, H.J., Pang, I.H., Shade, D., Wordinger, R.J., Yorio, T., Clark, A.F., Agarwal, N. 2001. Characterization of a transformed rat retinal ganglion cell line. Brain Res. Mol. Brain Res. 86. 1-12.

Lafuente, M.P., Villegas-Pérez, M.P., Sobrado-Calvo, P., García-Avilés, A., Miralles, de Imperial, J., Vidal-Sanz, M. 2001. Neuroprotective effects of alpha(2)-selective adrenergic agonists against ischemia-induced retinal ganglion cell death. Invest. Ophthalmol. Vis. Sci. 2001. 42, 2074-2084.

Leem, J.Y., Nishimura, C., Kurata, S., Shimada, I., Kobayashi, A., Natori, S. 1996. Purification and characterization of N-beta-alanyl-5-S-glutathionyl-3,4-dihydroxyphenylalanine, a novel antibacterial substance of Sarcophaga peregrina (flesh fly). J. Biol. Chem. 271.13573-13577.

Lim, J.H., Lee, J.C., Lee, Y.H., Choi, I.Y., Oh, Y.K., Kim, H.S., Park, J.S., Kim, W.K. 2006. Simvastatin prevents oxygen and glucose deprivation/reoxygenation-induced death of cortical neurons by reducing the production and toxicity of 4-hydroxy-2E-nonenal. J. Neurochem. 2006. 97, 140-150.

Maher, P., Hanneken, A. 2005. Flavonoids protect retinal ganglion cells from oxidative

stress-induced death. Invest. Ophthalmol. Vis. Sci. 46. 4796-4803.

Nakajima, Y., Inokuchi, Y., Nishi, M., Shimazawa, M., Otsubo, K., Hara, H. 2008. Coenzyme Q10 protects retinal cells against oxidative stress in vitro and in vivo. Brain Res. 2008. 1226. 226-233.

Nakajima, Y., Tsuruma, K., Shimazawa, M., Mishima, S., Hara, H. 2009. Comparison of bee products based on assays of antioxidant capacities. BMC Complement Altern. Med. 9. 1-9.

Nishikawa, T., Akiyama, N., Kunimasa, K., Oikawa, T., Ishizuka, M., Tsujimoto, M., Natori, S. 2006. Inhibition of in vivo angiogenesis by N-beta-alanyl-5-S-glutathionyl-3,4-dihydroxyphenylalanine. Eur. J. Pharmacol. 539. 151-157.

Pease, M.E., McKinnon, S.J., Quigley, H.A., Kerrigan-Baumrind, L.A., Zack, D.J., 2000. Obstructed axonal transport of BDNF and its receptor TrkB in experimental glaucoma. Invest. Ophthalmol. Vis. Sci. 41, 764-774.

Quigley, H.A., Nickells, R.W., Kerrigan, L.A., Pease, M.E., Thibault, D.J., Zack, D.J. 1995. Retinal ganglion cell death in experimental glaucoma and after axotomy occurs by apoptosis. Invest Ophthalmol Vis Sci. 1995 Apr;36(5):774-786.

Rao, N. A., Thaete, L.G., Delmage, J.M., Sevanian, A. 1985. Superoxide dismutase in ocular structures. Invest. Ophthalmol. Vis. Sci. 26. 1778-1781.

Rao, N. A. 1990. Role of oxygen free radicals in retinal damage associated with experimental uveitis. Trans. Am. Ophthalmol. Soc. 88, 797-850.

Shimazawa, M., Yamashima, T., Agarwal, N., Hara, H. 2005. Neuroprotective effects of minocycline against in vitro and in vivo retinal ganglion cell damage. Brain Res. 1053, 185-194.

Tatsumi, Y., Kanamori, A., Nagai-Kusuhara, A., Nakanishi, Y., Agarwal, N., Negi, A., Nakamura, M. 2008. Nipradilol protects rat retinal ganglion cells from apoptosis induced by serum deprivation in vitro and by diabetes in vivo. Curr. Eye Res. 33. 683-692.

Wadia, J.S., Chalmers-Redman, R.M., Ju, W.J., Carlile, G.W., Phillips, J.L., Fraser, A.D., Tatton, W.G. 1998. Mitochondrial membrane potential and nuclear changes in apoptosis caused by serum and nerve growth factor withdrawal: time course and modification by (-)-deprenyl. J. Neurosci. 18. 932-947.

Figure legends

Fig. 1. Protective effects of 5-S-GAD on RGC-5 cell death induced by hydrogen peroxide and serum deprivation treatments. Cell viability was estimated by the MTT assay. (A) RGC-5 cells were cultured with 5-S-GAD at 5-50 μM for 24 h. Hydrogen peroxide at 300-600 μM induces cell death of RGC-5 cells to 55% of the control level within 24 h. 5-S-GAD at 25-50 μM completely blocks the cell death induced by hydrogen peroxide. *$P<0.01$ vs. control cells; $^{+}P<0.01$ vs. hydrogen peroxide treatment (n=6). (B) Serum deprivation induces cell death to 35% of the control level. 5-S-GAD completely blocks the cell death induced by serum deprivation. *$P<0.01$ vs. control cells; $^{+}P<0.01$ vs. serum deprivation (n=6).

Fig. 2. Prevention of hydrogen peroxide-induced RGC-5 cell apoptosis by 5-S-GAD. (A-C) Nuclear condensation of RGC-5 cells revealed by Hoechst 33258 staining. (A) Control cells. (B) Cells treated with hydrogen peroxide (300 μM). (C) Cells treated with hydrogen peroxide (300 μM) plus 5-S-GAD (50 μM). Note the suppression of nuclear condensation by 5-S-GAD (C) compared with the hydrogen peroxide treatment (B). (D) Quantitative data for the cell numbers with positive staining. *$P<0.01$ vs. control cells; $^{+}P<0.01$ vs. hydrogen peroxide treatment (n=5). (E) DNA fragmentation in a 2% agarose gel. 5-S-GAD prevents the DNA laddering induced by hydrogen peroxide. Lane M: 100-bp markers; lane C: control cells; lane G: cells treated with 5-S-GAD; lane H: cells treated with hydrogen peroxide; lane HG: cells treated with hydrogen peroxide plus 5-S-GAD.

Fig. 3. Decrease of hydrogen peroxide-induced fluorescence intensity by 5-S-GAD. ROS levels in RGC-5 cells was evaluated by CM-H_2DCFDA staining (A, D, G). RGC-5 cell apoptosis was evaluated by staining with Hoechst 33258 (B, E, H). Merged images of CM-H_2DCFDA and Hoechst

33258 staining (C, F, I). (A-C) Control cells. (D-F) Cells treated with hydrogen peroxide. (G-I) Cells treated with hydrogen peroxide plus 5-S-GAD (50 μM). (J) Quantitative data for fluorescence intensity measured using a fluorescence plate reader. *P<0.01 vs. control cells; $^{+}$P<0.01 vs. hydrogen peroxide treatment (n=5).

Fig. 4. Prevention of serum deprivation-induced ROS production and DNA fragmentation by 5-S-GAD. RGC-5 cells were cultured under serum-free conditions with or without 5-S-GAD for 9 h. (A, D, G) CM-H_2DCFDA staining. (B, E, H) Hoechst 33258 staining. (C, F, I) Merged images of CM-H_2DCFDA and Hoechst 33258 staining. (A-C) Control cells. (D-F) Cells treated with serum deprivation. (G-I) Cells treated with serum deprivation plus 5-S-GAD (50 μM). (J) Quantitative data for ROS production measured using a fluorescence plate reader. *P<0.01 vs. control cells; $^{+}$P<0.01 vs. serum deprivation treatment (n=5). (K) DNA fragmentation in an agarose gel. Lane M: 100-bp DNA markers; lane C: control cells; lane G: cells treated with 5-S-GAD; lane S: cells treated with serum deprivation; lane SG: cells treated with serum deprivation plus 5-S-GAD.

Fig. 5. Prevention of hydrogen peroxide- and serum deprivation-induced 4-HNE production by 5-S-GAD. RGC-5 cells were cultured under hydrogen peroxide exposure or serum-free conditions with or without 5-S-GAD for 12 h. 4-HNE production was measured by dot blotting analyses with an anti-4-HNE antibody. 5-S-GAD blocks the increases in 4-HNE induced by hydrogen peroxide (A) and serum deprivation (B). Levels of β-actin bands were not changed during these treatments. *P<0.01 vs. control cells; $^{+}$P<0.01 vs. hydrogen peroxide or serum deprivation treatment (n=5).

Fig. 6. Activation of anti-apoptotic proteins in RGC-5 cells induced by 5-S-GAD. Apoptotic or anti-apoptotic proteins in RGC-5 cells treated with hydrogen peroxide or hydrogen peroxide plus

5-S-GAD were analyzed by western blotting. (A) Bax. 5-S-GAD restores the increase in Bax induced by hydrogen peroxide treatment (upper bands). *P<0.01 vs. control cells; +P<0.01 vs. hydrogen peroxide treatment (n=3). β-Actin remains unchanged by the treatments (lower bands). (B) Caspase-3. 5-S-GAD restores the increase in caspase-3 induced by hydrogen peroxide treatment. *P<0.01 vs. control cells; $^{+}$P<0.01 vs. hydrogen peroxide treatment (n=3). (C) Akt. 5-S-GAD restores the decrease in phospho-Akt induced by hydrogen peroxide to the control level (upper bands). Note the induction of phospho-Akt by 5-S-GAD alone. *P<0.01 vs. control cells; $^{+}$P<0.01 vs. hydrogen peroxide treatment (n=3). Akt remains unchanged by any of the treatments (lower bands). (D) Bcl-2. 5-S-GAD restores the decrease in Bcl-2 induced by hydrogen peroxide treatment. Note the induction of Bcl-2 by 5-S-GAD alone. *P<0.01 vs. control cells; $^{+}$P<0.01 vs. hydrogen peroxide treatment (n=3).

Figure

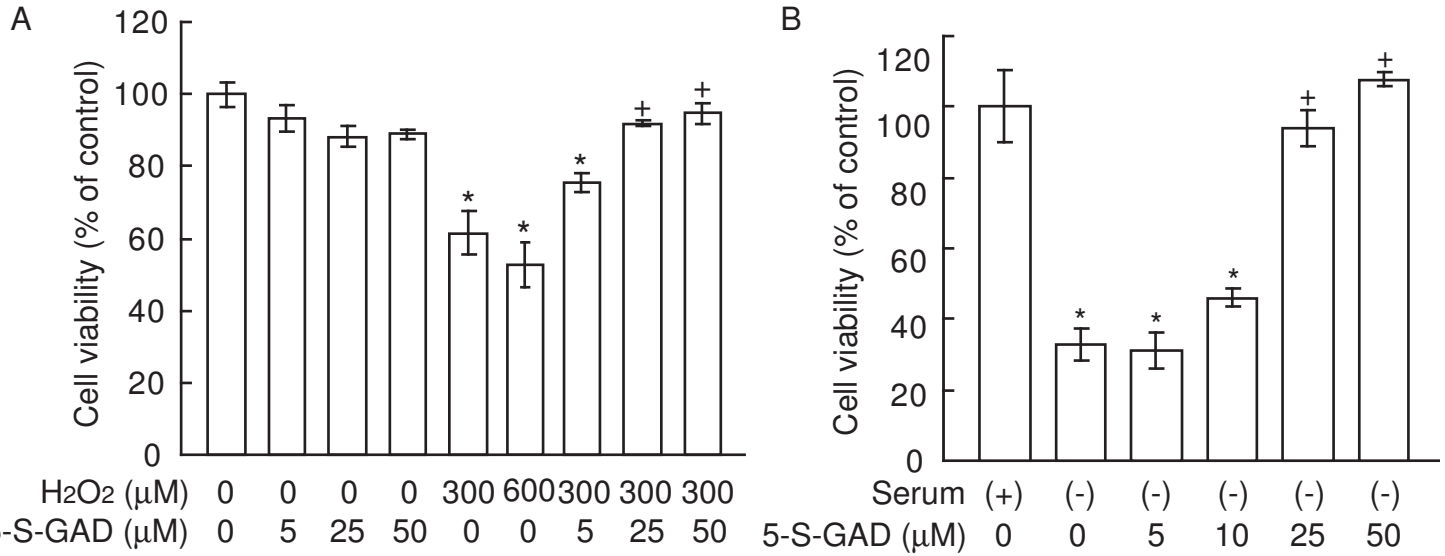
A
Cell viability (% of control)
120
100
80
60
40
20
0
H2O2 (μM) 0 0 0 0 300 600 300 300 300
5-S-GAD (μM) 0 5 25 50 0 0 5 25 50
B
Cell viability (% of control)
120
100
80
60
40
20
0
Serum (+) (-) (-) (-) (-) (-)
5-S-GAD (μM) 0 0 5 10 25 50

Figure

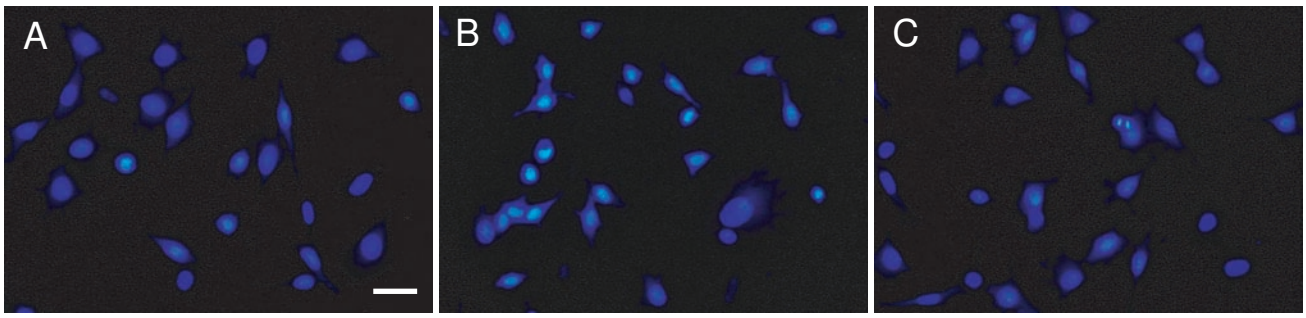
A
B
C

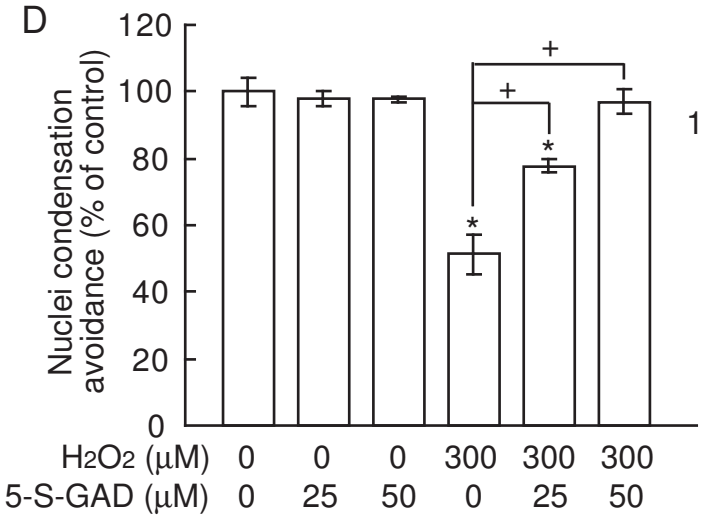
D
Nuclei condensation avoidance (% of control)
120
100
80
60
40
20
0
H2O2 (μM) 0 0 0 300 300 300
5-S-GAD (μM) 0 25 50 0 25 50
+
+
*
*

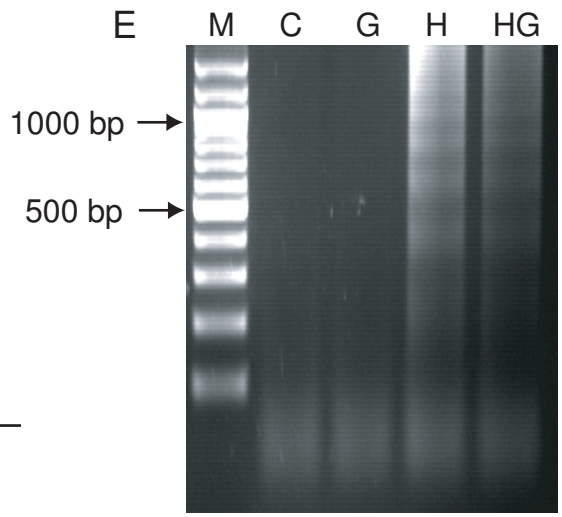
E
M C G H HG
1000 bp
500 bp

Figure

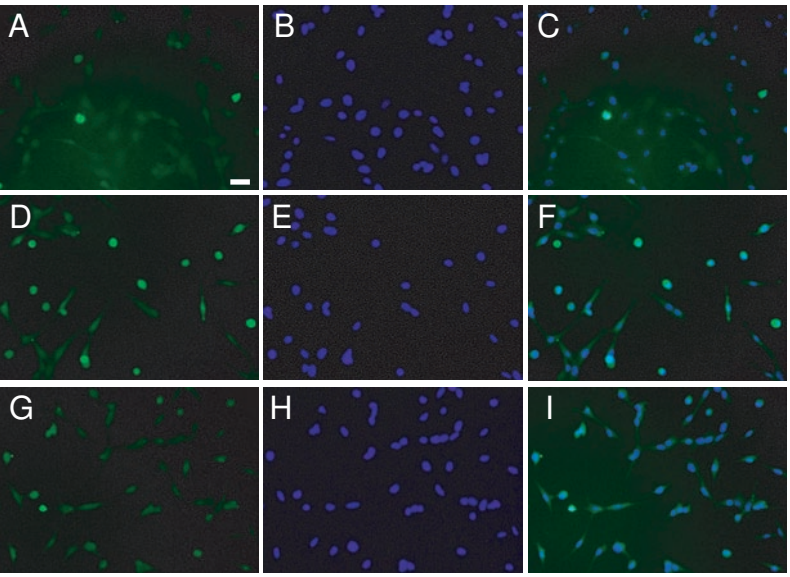
A
B
C
D
E
F
G
H
I

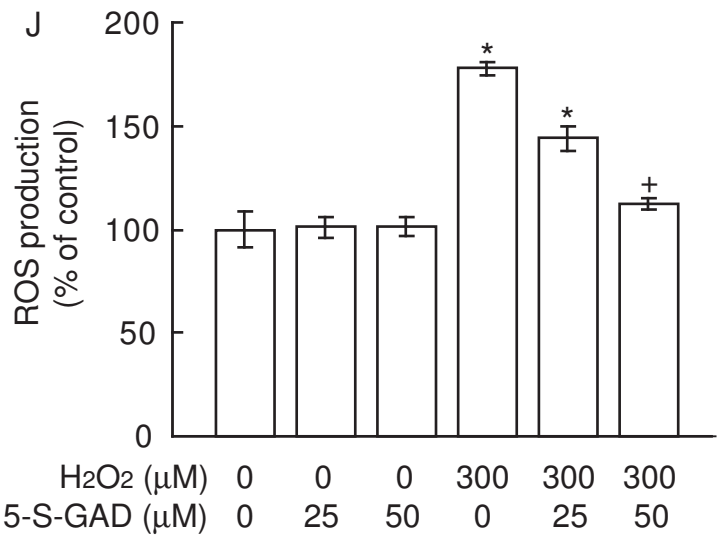
J
ROS production
(% of control)
200
150
100
50
0
*
*
+
H2O2 (μM) 0 0 0 300 300 300
5-S-GAD (μM) 0 25 50 0 25 50

Figure

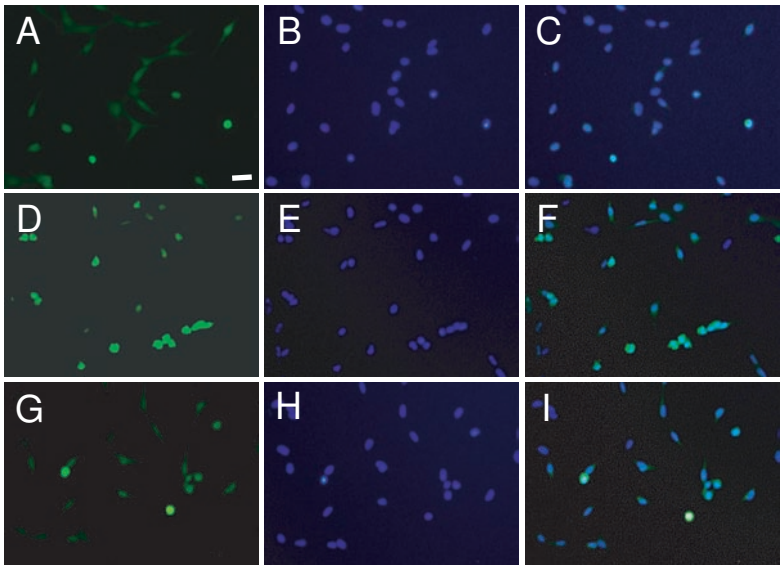
A
B
C
D
E
F
G
H
I

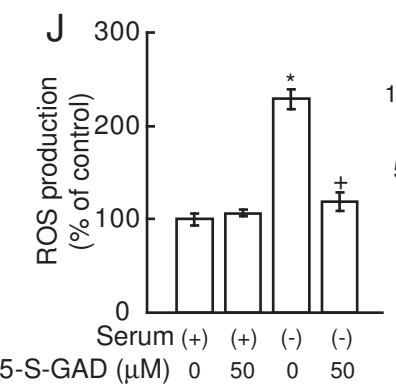
J
300
200
100
0
ROS production
(% of control)
*
+
Serum (+) (+) (-) (-)
5-S-GAD (μM) 0 50 0 50

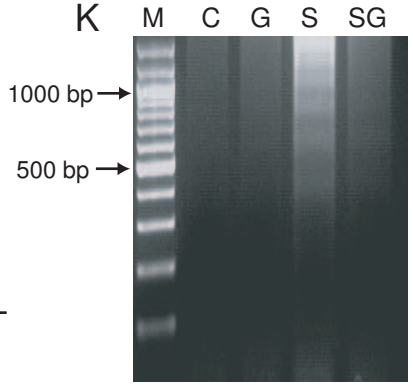
K
M C G S SG
1000 bp
500 bp

Figure

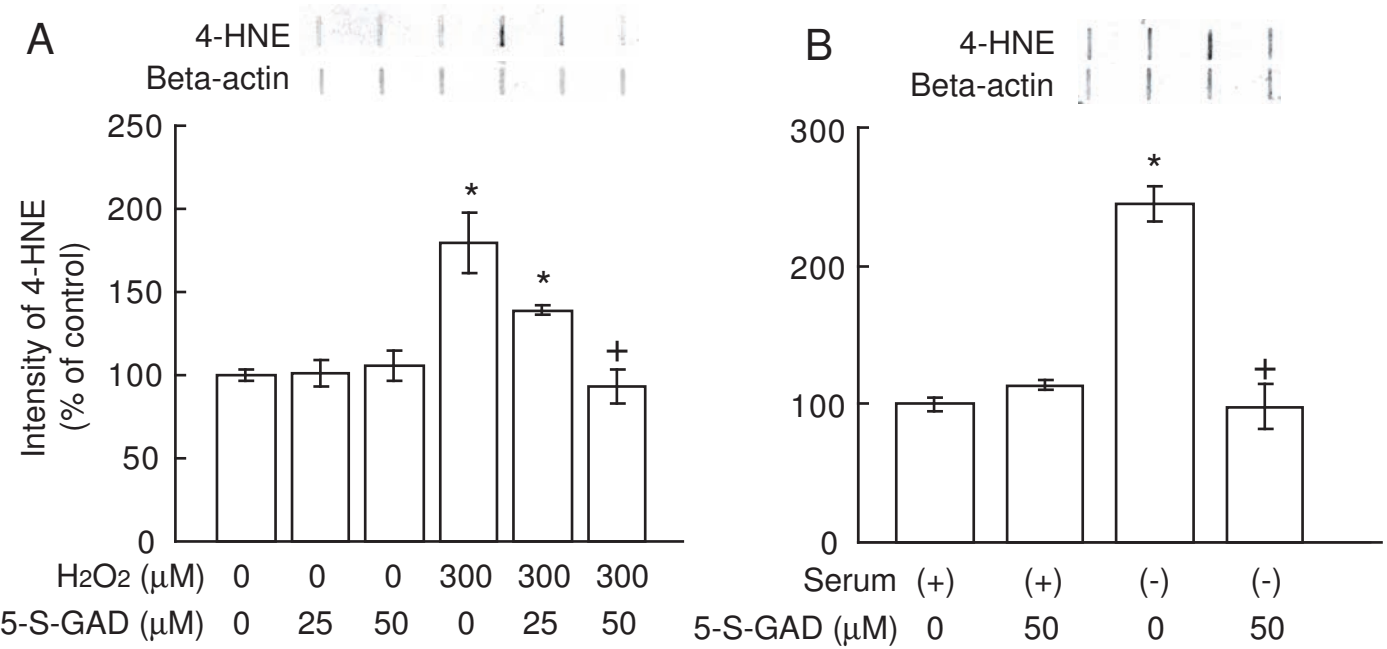
A
4-HNE
Beta-actin
Intensity of 4-HNE (% of control)
250
200
150
100
50
0
H2O2 (μM) 0 0 0 300 300 300
5-S-GAD (μM) 0 25 50 0 25 50
B
4-HNE
Beta-actin
300
200
100
0
Serum (+) (+) (-) (-)
5-S-GAD (μM) 0 50 0 50

Figure

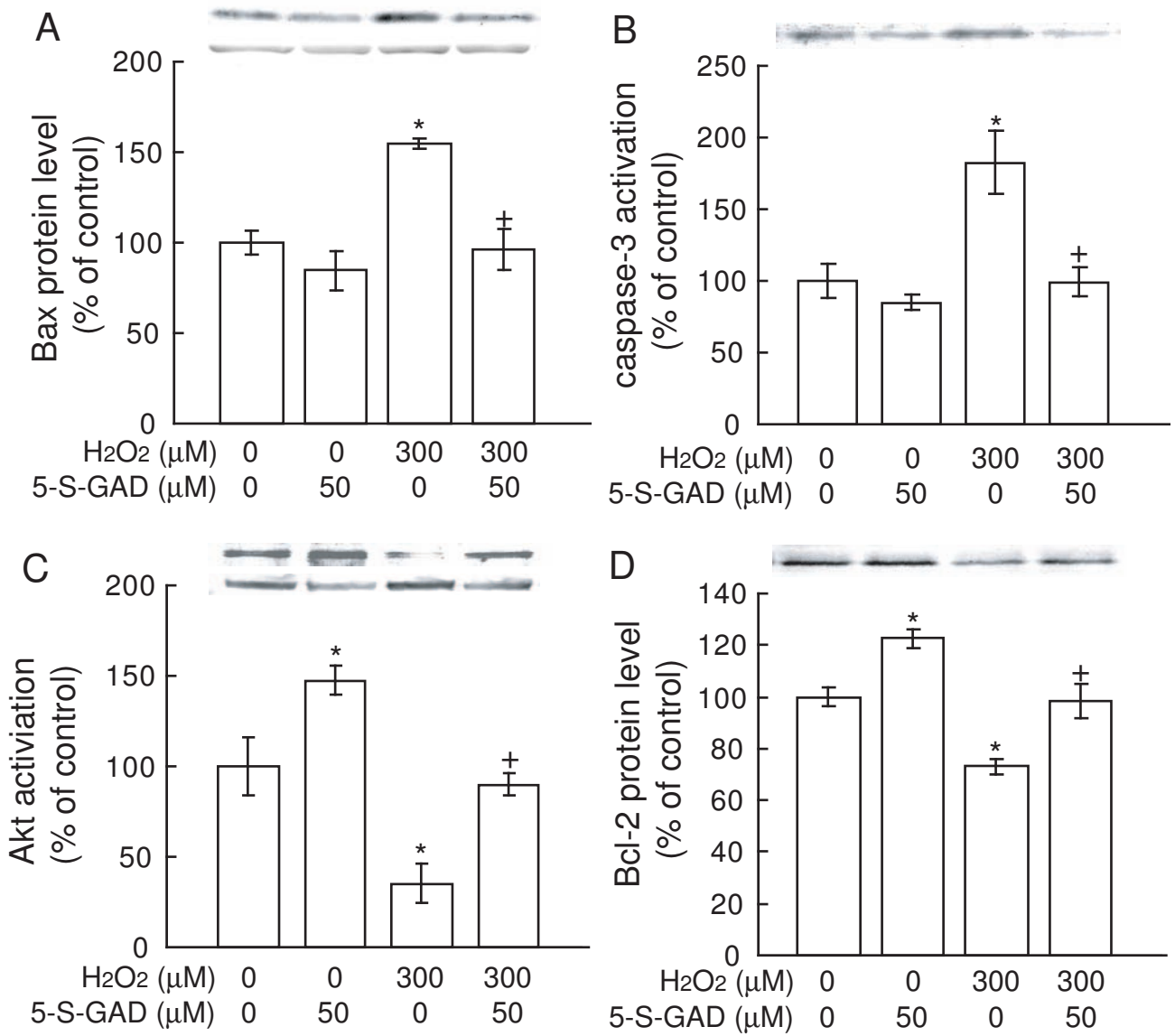
A
Bax protein level (% of control)
200
150
100
50
0
*
‡
H2O2 (μM) 0 0 300 300
5-S-GAD (μM) 0 50 0 50
B
caspase-3 activation (% of control)
250
200
150
100
50
0
*
‡
H2O2 (μM) 0 0 300 300
5-S-GAD (μM) 0 50 0 50
C
Akt activiation (% of control)
200
150
100
50
0
*
*
‡
H2O2 (μM) 0 0 300 300
5-S-GAD (μM) 0 50 0 50
D
Bcl-2 protein level (% of control)
140
120
100
80
60
40
20
0
*
*
‡
H2O2 (μM) 0 0 300 300
5-S-GAD (μM) 0 50 0 50